NMR-based metabolomics approach on optimization of malolactic fermentation of sea buckthorn juice with *Lactiplantibacillus plantarum*

N. Markkinen [*], R. Pariyani, J. Jokioja, M. Kortesniemi, O. Laaksonen, B. Yang

Food Chemistry and Food Development, Department of Life Technologies, University of Turku, FI-20014 Turun yliopisto, Finland

ARTICLE INFO

ABSTRACT

This work investigated the impact of malolactic fermentation on the metabolomic profile of sea buckthorn juice to optimize the fermentation process for flavor modification. Six strains of *L. plantarum* were used with varied pH of the juice, cell acclimation, and fermentation time. [1]H-NOESY spectra were acquired from fresh and fermented juices with a total of 46 metabolites identified. Less sugars and quinic acid were metabolized at pH 2.7 while oxidation of ascorbic acid was reduced at pH 3.5. L-Malic acid, essential amino acids, and nucleosides were consumed early during fermentation while sugars in general were consumed later in the fermentation. If deacidification is the main target of fermentation, strains that produce less acids and ferment less sugars, shorter fermentation time, and lower starter pH should be used. Higher starter pH and longer fermentation time promote formation of antimicrobial compounds and potentially increase antioxidant stability.

1. Introduction

Malolactic fermentation is a method often applied as a secondary fermentation to wines with high acidity to reduce sour notes and to modify *bouquet* of the wine (Brizuela et al., 2019). Recent studies show that the method can be utilized also for development of non-alcoholic beverages to naturally improve e.g. flavor or shelf-life (Di Cagno et al., 2011; Filannino, Cardinali, et al., 2014; Filannino, Cagno, et al., 2016; Tomita et al., 2017). One potential candidate for bioprocessing with malolactic fermentation is sea buckthorn (*Hippophaë rhamnoides*) juice, as it has low sensory value due to intense acidity and astringency. The rationale behind developing sea buckthorn products is the increased consumer interest towards its benefits on skin and cardiovascular health (Bal et al., 2011). Earlier work has shown that sea buckthorn is a promising target for malolactic fermentation with *Lactiplantibacillus plantarum* (Markkinen et al., 2019, Markkinen et al., 2021). However, further investigations are required to unveil metabolic responses of *L. plantarum* in sea buckthorn juice (SBJ) in relation to various fermentation factors, which would allow for more effective product

development of fermented beverages from acidic fruit and berry materials.

Optimization of the fermentation process requires understanding of the chemical composition of the raw material, as lactic acid bacteria utilized in malolactic fermentation require an energy source, nitrogen source, essential amino acids, nucleosides, and certain minerals for an effective fermentation. On the other hand, antimicrobial compounds (e. g., ethanol or phenolics), temperature, pH, and salinity among other factors affect gene expression and metabolic activity of the fermenting organism, which in turn have an impact on how texture, taste, aroma, and functional properties are developed during fermentation (Di Cagno et al., 2011; Filannino, Cagno, et al., 2016; Huang et al., 2020; Wei et al., 2018). Therefore, holistic analytical tools that allow both prescreening of the raw material as well as detecting complex chemical changes during the fermentation are required. In this work, NMR-based (nuclear magnetic resonance spectroscopy) metabolomics was selected for this purpose.

Earlier, NMR metabolomics have been applied to profile wine metabolites in relation to fermentation factors (Hong, 2011), to monitor

---

metabolic changes in natural spoilage of mango juice (Duarte et al., 2006), in fermentation of vegetable juice with various *Lactobacillus* spp. (Tomita et al., 2017), and in fermentation of cantaloupe and dragon fruit juices with *L. plantarum* (Muhialdin et al., 2020; Muhialdin et al., 2021). In the two latter cases, fermentation with *L. plantarum* improved shelf-life and sensory value of both juices. Related to sea buckthorn berries, NMR metabolomics has been utilized to evaluate berry quality (Li et al., 2013), discriminate sea buckthorn from other species belonging to the *Hippophaë* genus (Liu et al., 2017) and to identify the metabolites in relation to subspecies, cultivar and growth locations (Kortesniemi et al., 2014, 2017). However, no research currently exists that has investigated the optimization of malolactic fermentation of SBJ using NMR. In our current work, NMR-based metabolomics is combined with multivariate and univariate statistical methods for finding associations between non-volatile metabolites in fermented SBJ and juice pH (2.7 and 3.5), acclimation (with or without), fermentation time (36 h and 72 h), and *L. plantarum* strain. The goal was to seek out combinations that promote beneficial flavor development (i.e., malolactic conversion without sugar fermentation, phenolic metabolism) or other potential benefit, such as formation of bioactive or antimicrobial compounds. At the same time, we seek out to reveal how chemical changes during fermentation are interlinked and to present metabolic systems of *L. plantarum* that are responsible for the formation or removal of individual metabolites.

1.1. Hypotheses

NMR-based metabolomics reveals phenotypical variation in malolactic fermentation, sugar utilization, organic and amino acid metabolism, and secondary metabolite modification between various strains of *L. plantarum* in fermentation of acidic fruit material.

2. Materials and methods

2.1. Berry material

Frozen sea buckthorn (*Hippophaë rhamnoides* subsp. *mongolica*, mixture of cultivars 'Ljubitelskaja' and 'Prozrachnaya') berries were purchased from a professional farmer (Vinkkilän luomutuote, Vehmaa, Finland). The berries were stored at −20 °C until use.

2.2. Juice preparation

SBJ was prepared for fermentation as described earlier (Markkinen et al., 2021). Frozen berries of sea buckthorn were microwaved at 600 W for 3.5 min. Berries were made into a mash with a Bamix immersion blender and fruit press (Chef Titanium XL with AT644 attachment, Kenwood, UK) was used to extract the juice. The extraction of the juice was performed in batches of ~ 400 g, and the juice solids were removed with cheesecloth. Juice batches were pooled, divided into aliquots, and stored at −20 °C until use.

Two different starter pH values were used, natural pH (2.7) and adjusted pH (3.5). Juice at natural pH was diluted with distilled water 1:1 (w/w), while juice with adjusted pH was prepared by first adding distilled water (approximately 40% (w) of the mass of the undiluted juice), pH adjusted to 3.50 ± 0.05 with 1 M NaOH, and finally adding dH$_2$O to reach dilution of 1:1 (w/w). As SBJ has relatively high oil content and high turbidity, measuring mass instead of volume for dilution and pH adjustment was more convenient.

After dilution, juices were divided to 30 mL aliquots, and to remove natural microflora, the juice samples were pasteurized in a water bath (temperature ~ 96 °C) until the juice temperature reached 90 °C. After pasteurization, samples were cooled in an ice batch. Pasteurization was monitored with a thermometer (TM-947SD, Lutron Electronics, South Korea) coupled with a thermocouple probe. Pasteurized juice samples were tempered for 1 h at + 30 °C in an IF-110Plus incubator (Memmert GmbH, Schwabach, Germany) prior inoculation.

2.3. Revival of freeze-dried cultures and glycerol stock preparation

Freeze-dried cultures of fives strains of *Lactiplantibacillus plantarum* (old name *Lactobacillus plantarum* subsp. *plantarum*) (DSM 1055 (isolated from bread dough), DSM 100813 (grape must), DSM 10492 (olive brine), DSM 13273 (jojoba meal fermentation), and DSM 20174^T (pickled cabbage)) and one strain belonging to *Lactiplantibacillus argentoratensis* (old name *Lactobacillus plantarum* subsp. *argentoratensis*) (DSM 16365^T, fermented cassava roots) were obtained from Deutsche Sammlung von Mikroorganismen und Zellkulturen (DSMZ, Braunschweig, Germany). Lyophilized cultures were revived according to manufacturer guidelines in De Man, Rogosa and Sharpe (MRS, LabM, Heywood, UK) plates for 48 h at 30 °C, followed by a transfer of a single colony to 250 mL of general edible medium (*GEM*), prepared according to a previous report (Markkinen et al., 2019) with modifications (dextrose, 30 g/L; soy peptone, 20 g/L; yeast extract, 7 g/L; MgSO$_4$ × 7 H$_2$O, 1 g/L; MnSO$_4$ × H$_2$O, 0.05 g/L; in potassium phosphate buffer 0.01 M, pH 6.3 ± 0.2). Cell culture was incubated at 30 °C for 24 h, mixed with 20 % glycerol solution (1:1, v/v), and stored as aliquots at −80 °C until use.

2.4. Optical density (OD$_{600}$) linear regression models for estimating cell counts

Optical density (OD$_{600}$) linear regression models were prepared to standardize the inoculation rate of the SBJ individually for each of the strains used in this work. Early stationary phase was reached after approximately 24 h of fermentation with the average cell count of 1–3 × 10^9 CFU/mL, corresponding to OD$_{600}$ = 2.2–2.3 (UV/Vis UV3100PC, VWR, PA, USA). Linear range of OD$_{600}$ used in the study was 0.2–0.7, corresponding to dilutions 1:30–1:6 of overnight culture. Sterile *GEM* media was used as a blank sample. Five dilutions between 0.2 and 0.7 of OD$_{600}$ were enumerated with viable colony count (see Section 2.7) to produce linear regression model for each strain to estimate cell count in starter cultures used in SBJ inoculation.

2.5. Acclimation medium

Composition of cell acclimation medium (*CAM*) was the same as *GEM* (Section 2.3) with additional 4 g/L of L-malic acid. However, pH of *CAM* was adjusted to 4.5 instead of 6.3. Overnight cultures were started with a single colony from a MRS plate, similarly to inoculation of *GEM*.

2.6. Starter culture preparation and fermentation

First, a scrape from the glycerol stock was cultured in an MRS plate for 36–48 h at 30 °C. Next, a single colony was transferred to 250 mL growth medium (*GEM* or *CAM*). After incubation at 30 °C for 24–25 h, cells were collected from 80 to 90 mL of the inoculate by centrifugation (4500×*g*, 5 min, 20 °C). To remove residual medium, cells were washed twice with phosphate buffered saline (PBS, pH 7.4). After removing supernatant, cells were re-suspended to 5 mL of PBS. To estimate the cell count of the cell concentrate, OD$_{600}$ was measured from a 1:200 dilution. Cell concentrate was added to 30 mL of pasteurized SBJ (pH 2.7 or pH 3.5) to reach an estimated initial cell count of 2 × 10^8 CFU/mL juice. Cell count of the starter culture was confirmed with viable colony count (see Section 2.7). All fermentations were prepared as biological triplicates (three parallel inoculations). The fermentation temperature was 30 °C for all strains, and juice were incubated either for 36 or 72 h. Control samples were prepared and fermented similarly as described above but without the addition of microbes. After the incubation period, metabolic activity was halted by cooling samples in an ice bath. Each sample was divided into aliquots and stored at −80 °C until analysis.

2.7. Viable colony count

Cell suspension was first serially diluted (1/10) with PBS until expected cell count was 300–3000 CFU/mL. This dilution as well as one magnitude more concentrated and one magnitude more diluted cell cultures were used for viable plate count. From all three dilutions, 100 μL of cell culture was streaked on individual MRS agar plates, followed by incubation at 30 °C for 36–48 h. All plates were prepared in triplicates. Colony counts between 30 and 300 on each plate were considered acceptable for enumeration.

2.8. NMR sample preparation and spectral acquisition

To remove residual and microbial solids and lipids, the thawed juice samples were first centrifuged at $14000 \times g$ for 3 min at 4 °C, and 500 μL of the supernatant was further clarified by centrifugal filtration (0.45 μm nylon membrane, VWR, Radnor, PA, USA). Next, 300 μL of the filtrate, 70 μL of 1.5 M KH_2PO_4 buffer (pH 6.50 ± 0.10), 70 μL of Chenomx-ISTD (5 mM DSS-d_6, 0.1% w/v sodium azide, pH 7.0, in D_2O; Chenomx Inc., Edmonton, AB, Canada) and 300 μL of reverse-osmosis water were combined. The pH was adjusted to 6.50 ± 0.01 with either HCl or NaOH, and the sample transferred into a 5 mm NMR tube. Spectra were recorded using 600 MHz AVANCE-III NMR-system (Bruker Biospin, Rheinstetten, Germany) equipped with CryoProbe Prodigy TCI (Bruker Biospin) and an automated sample changer SampleJet. Instrument was operated using Topspin (version 4.1.0) and IconNMR softwares (Bruker Biospin). Proton spectra were acquired at 298.2 K with 1D NOESY pulse program with presaturation (*noesygppr1d*). A single NMR sample was prepared from each biological replicate for the analyses. The following parameters were used: size of the FID, 64 k; spectral width, 14 ppm; number of scans, 128; number of dummy scans, 4; 90° proton pulse length 10.98 μs; relaxation delay, 5 s; mixing time, 0.10 s. Multiplicity edited ^{1}H–^{13}C heteronuclear single quantum coherence (HSQC) spectrum using echo/antiecho detection and gradient pulses (*hsqcedetgpsisp2.3*) was acquired with the following parameters: 90° pulse values, 8 μs (proton) and 15 ls (carbon); relaxation delay, 2 s; spectral width, 165 ppm (f1) and 16 ppm (f2); data points, 256 increments of 2 k; number of scans, 32. ^{1}H–^{13}C heteronuclear multiple-bond connectivity (HMBC) spectrum with absolute value detection (*hmbcgplpndqf*) was acquired with the parameters: spectral width, 220 ppm (f1) and 10 ppm (f2); data points, 128 increments of 2 k; number of scans, 64. Homonuclear ^{1}H–^{1}H COSY spectrum (*cosygpppqf*) was acquired with 2048 data points with increments of 128 and with 16 scans.

2.9. NMR data processing and statistical analyses

Acquired spectra were processed (phase and baseline corrections, line broadening) using Chenomx NMR Suite software (version 8.6, Chenomx Inc., Edmonton, AB, Canada). For chemical shift referencing, the methyl group of the internal standard DSS was used (0.00 ppm for both ^{1}H and ^{13}C). The processed spectra were divided into 0.02 ppm-sized bins, water region removed, and the data normalized to the total spectral area. To align the spectral data for untargeted statistical analyses, dataset was imported into MATLAB software (version 2020B, Mathworks Inc., Natick, MA, USA) and processed using the *icoshift* algorithm.

Principal component analysis and orthogonal principal least squares discrimination (OPLS-DA) of processed and aligned spectra were carried out using SIMCA (version 16, Umetrics, Umeå, Sweden). Pareto scaling and mean centering were applied to the datasets. The validation of the OPLS-DA models was performed with internal validation of 200 permutations, determining explained variation (R^2Y_{cum}) and predictive ability (Q^2Y_{cum}) and with analysis of variance of cross-validated residuals (CV-ANOVA; *p*-value < 0.05 considered significant).

Metabolite annotation was based on chemical shift, *J*-coupling, heteronuclear coupling (HSQC, HMBC), and homonuclear coupling

(^{1}H–^{1}H COSY). Spectrum databases of Chenomx NMR Suite software, the Human Metabolomics Database (http://www.hmdb.ca/) and the Biological Magnetic Resonance Data Bank (http://www.bmrb.wisc.edu/) were used as the main references in addition to other literature sources (Duarte et al., 2006; Kortesniemi et al., 2017; Tomita et al., 2017). Selected compounds were identified using authentic standards.

Quantification of selected metabolites were performed with Chenomx NMR Suite using integral value of the methyl signal of DSS-d_6 (0.5 mM) at 0 ppm as reference. Known concentration of internal standard (maleic acid, 1 mM) was used as a correction factor to normalize data. For compounds not existing in the Chenomx compound library, results were normalized using the total peak area.

To compare metabolic responses based on the starter pH of SBJ, hierarchical clustering heatmap analysis was performed with MetaboAnalyst 5.0 open source platform (https://www.metaboanalyst.ca/) (Chong and Xia, 2018). Data was normalized with auto-scaling.

Results of quantified metabolites were presented as average ± standard deviation. Paired *t*-test was used to compare the means of individual metabolites, grouped by growth medium with fermentation time and the starter pH set as constant (72 h and 3.5, respectively). To determine the contribution of each fermentation variable (strain, pH, medium, time) to the variance of the individual metabolites, general linear model was calculated with IBM SPSS Statistics (Version 27) using data from samples where fermentation was successful (i.e. fermentation of L-malic to L-lactic acid was detected). For multiple comparisons between *L. plantarum* strains and the means of individual metabolites, Tukey's test for population with equal variances and one-way ANOVA were performed, for which R version 4.0.4 (R Core Team, 2021) with package *multcompView* was utilized. Pearson's correlations of concentrations between selected metabolites were calculated using Microsoft Excel. For illustration of the results, the data was first processed with R packages *dplyr* and *tidyr* and then visualized with package *ggplot2* to present metabolic responses of *L. plantarum* in SBJ based on fermentation time, growth medium, and microbial strain. Details of the R packages used in this work are listed in Supplementary Table S1.

3. Results and discussion

3.1. Identification of metabolites from fresh and fermented sea buckthorn juices

In total 46 metabolites were identified from either fresh or fermented SBJ (Supplementary Table S2). These include amino acids, fruit acids, ketoacids, mono- and disaccharides, ketones, nucleosides, and one alkaloid, trigonelline. Earlier ^{1}H NMR analyses of sea buckthorn berry (Kortesniemi et al., 2014, 2017) and authentic standards allowed the identification of signals related to L-quebrachitol and ethyl-*O*-β-D-glucopyranoside (referred as ethyl glucose here on out). One unknown fermentation-related metabolite was determined as 3,4,5-trihydroxycyclohexane-1-carboxylic acid (3,4,5-OH-CHCA), earlier detected in spoiled mango juice (Duarte et al., 2006). However, another compound assumed as quinic acid metabolite remained unidentified (Supplementary Table S2). Based on the 1D NOESY spectra of fresh SBJ, main acids detected in the juice samples were L-malic acid and quinic acid, main sugars glucose, fructose, ethyl glucose, L-quebrachitol, main amino acids asparagine and alanine, and the most abundant alcohol ethanol. ^{1}H NMR profile of fresh SBJ was in accordance with earlier reports (Supplementary Fig. S1) (Kortesniemi et al., 2014, 2017; Li et al., 2013; Liu et al., 2017).

3.2. Metabolic responses of L. plantarum during fermentation

The scores plot of the principal component analysis of all collected data (Fig. 1A) showed the formation of two clear separate clusters along the first principal component (PC-1), which explained 86.6% of the variance. The separation was based on the level of metabolic activity
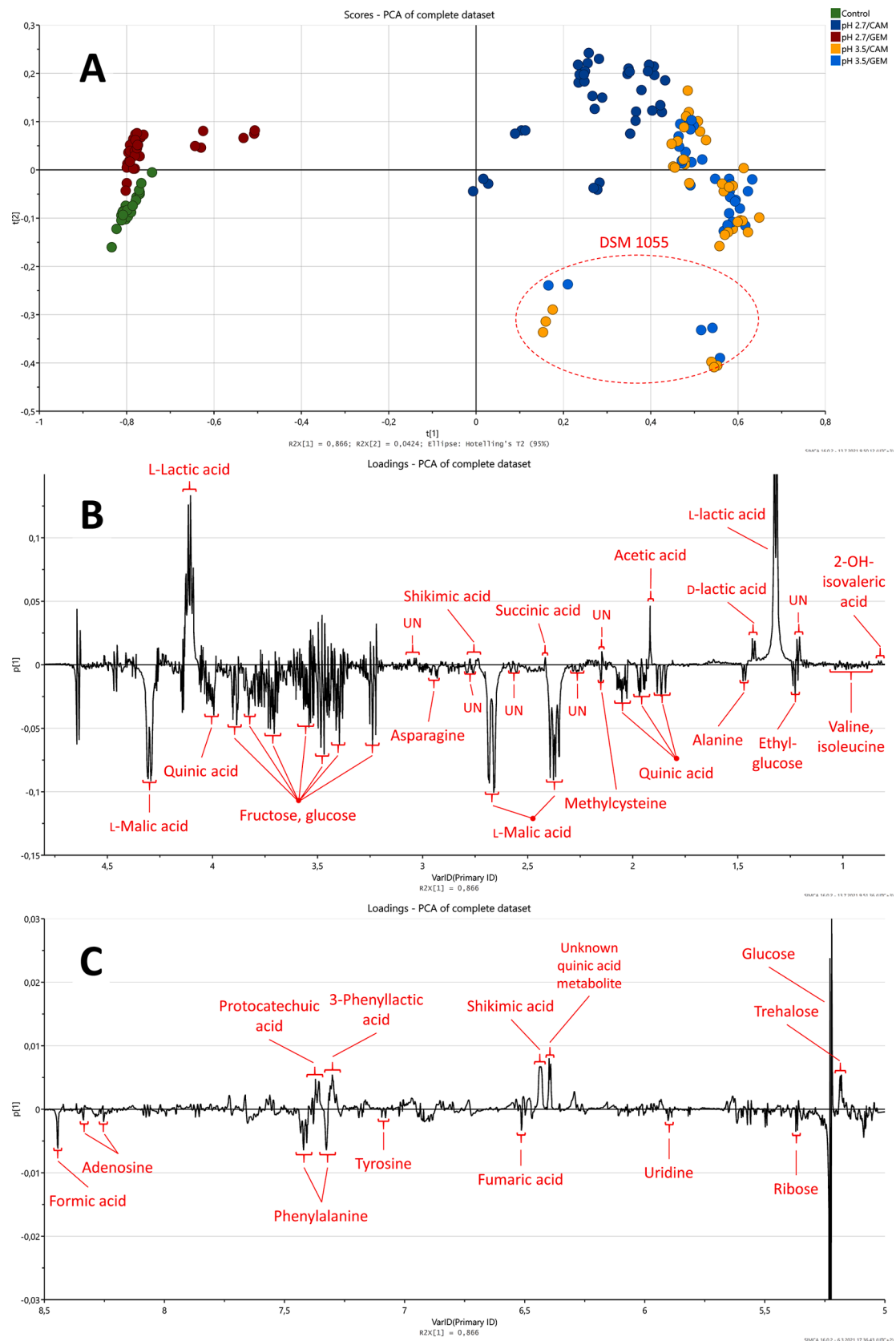
Fig. 1. Principal component analysis (PCA) scores plot (A) and correlation loadings plots (B: aliphatic region, C: aromatic region) based on the binned and aligned spectral data (4499 *X*-variables) of both non-treated sea buckthorn juice and juice fermented with *L. plantarum* (168 samples). A separate cluster marked with a dashed circle relate to samples fermented with strain DSM 1055.

during fermentation, with fermented juices appearing at the positive end of PC-1 and the control juice and the juice inoculated at pH 2.7 at the negative side. Little or no metabolic activity was observed in control juices without inoculation as well as in the inoculated juices with the initial pH of 2.7 and *GEM* as the growth medium. However, when the initial pH was was adjusted to 3.5 or cell acclimation was used (growth medium *CAM*) prior to inoculation, *L. plantarum* cells were able to ferment the raw material.

Within the positive end of PC-1 (i.e., the samples with signs of fermentation), *pH2.7/CAM* samples are separated from the *pH3.5/GEM* and *pH3.5/CAM* samples, while there was no clear separation between the two latter. This observation agrees with our earlier report regarding volatile composition of fermented SBJs (Markkinen et al. 2021). Within PC-2, one strain (DSM 1055) is clearly separated from the others at both pH 2.7 and pH 3.5. The differences in metabolic profiles based on starter pH and bacterial strain are discussed later (Sections 3.3 and 3.4, respectively).

From the loadings plot (Fig. 1B, C) it can be observed that higher intensity of the main signals of L-lactic, acetic, and succinic acids were observed from fermented samples while signals related to L-malic, quinic, formic and fumaric acids and sugars were higher with fresh SBJ. At the same time, the signals of ketoacids 2-hydroxyisovaleric acid and 3-phenyllactic acid (3-PLA) derived *via* transamination from valine and phenylalanine (Filannino, Cardinali, et al., 2014; Lavermicocca et al., 2003), respectively, were increased in fermented juices compared to control.

Free amino acids (methylcysteine, valine, isoleucine, alanine, tyrosine, and phenylalanine) were negatively associated with fermentation. *L. plantarum* typically lacks the enzymes to break down larger polypeptides, and thus smaller peptides and free amino acids are crucial for successful fermentation (Filannino, Cagno, et al., 2016; Ma et al., 2016). Optimization of milk fermentations with *L. plantarum* revealed six key amino acids, isoleucine, leucine, valine, tyrosine, methionine, and phenylalanine (Ma et al., 2016), of which all, except for methionine, were detected in SBJ and also consumed by *L. plantarum*. Transcriptomic analysis has revealed that genes associated with D-alanine metabolism and branched chain amino acid (BcAA) transport were upregulated in *L. plantarum C*2 during adaptation to acidic pineapple juice (pH = 3.7) (Filannino, Cagno, et al., 2016). On the other hand, metabolomic analysis using the same strain and raw material showed reduction in the BcAA content during fermentation but an increase during storage at + 4 °C (Filannino, Cardinali, et al., 2014). However, it should be noted that 2-hydroxyisovaleric acid is a common component in volatile esters of SBJ, and thus, an increase in 2-hydroxyisovaleric acid could derive from hydrolysis of the esters as well (Markkinen et al., 2021). Increase in shikimic and protocatechuic acids during fermentation was likely due to metabolism of quinic acid by *L. plantarum* (for more details, see Section 3.4).

Antifungal properties of 3-phenyllactic acid (3-PLA) have been evaluated earlier, showing potential as a natural antimicrobial agent (Dal Bello et al., 2007). Additionally, the antimicrobial activity of 3-PLA is augmented by both lactic and acetic acid (Lavermicocca et al., 2003). It can be speculated that malolactic fermentation could improve the shelf-life of SBJ by removing an energy source (i.e., L-malic acid) while increasing the contents of antimicrobial compounds, which in this case are lactic acid, acetic acid, and 3-PLA. Earlier, the fermentation of cantaloupe juice with *L. plantarum* FBS05 extended the shelf-life for six months (Muhialdin et al., 2021).

3.3. Effect of juice starter pH on the metabolic activity of L. plantarum

As seen in the PCA scores plot (Fig. 1A), *pH 2.7/GEM* samples made a separate cluster from *pH3.5/GEM* and *pH3.5/CAM* along the first principal component. The OPLS-DA model comparing the fermented samples with pH as class variable showed good fitness ($R^2Y_{cum} = 0.969$) and high predictive value ($Q^2Y_{cum} = 0.961$). The groups were significantly

separated (CV-ANOVA *p*-value = 2.15×10^{-21}) and Y-intercepts of R^2Y and Q^2Y were below 0.3 and 0.05, respectively, thus validating the model (Supplementary Fig. S2). General linear model analysis showed that starter pH contributed the most in the variance of concentrations of amino acids and amino acid-related metabolites, shikimic acid, succinic acid, and L-lactic acid (Supplementary Table S3). To further illustrate the compounds that were metabolized differently based on juice pH, hierarchical clustering heatmap analysis was used with selected metabolites (Fig. 2).

L-Malic acid, nucleosides, phenylalanine, and tyrosine were consumed by *L. plantarum* at comparable levels at both pH 2.7 and pH 3.5. However, branched chain amino acid and alanine metabolism was lower at pH 2.7 compared to pH 3.5. Additionally, secondary metabolite metabolism was increased at pH 3.5, shown as the higher formation of 3,4,5-OH-CHCA, shikimic acid, catechol, and protocatechuic acid during fermentation compared to metabolism at pH 2.7. Metabolism of sugars (i.e. glucose and fructose) was limited at native pH of SBJ in accordance with our earlier report (Markkinen et al., 2019). The formation of ethanol, acetoin and acetate was decreased at pH 2.7 compared to pH 3.5. Earlier, fermentation of bog bilberry juice with *L. plantarum* strains B7 and C8-1 showed higher formation of shikimic and acetic acid when juice pH was adjusted to 3.50 from 2.65, similar to our findings. However, contrary to the results in the current work, the same study reported higher rate of sugar utilization at lower pH (Wei et al., 2018).

In *L. plantarum*, fermentation of sugars to lactic acid is substantially reduced once extracellular pH reaches below 4 to avoid over-acidification of the growth substrate (Fernandez et al., 2008). Therefore, downregulation of the lactic acid forming pathway of glycolysis could explain why less sugars were fermented at lower pH in SBJ. On the other hand, *L. plantarum* possesses a pathway to maintain pH homeostasis by converting pyruvate to acetoin instead of lactate (Tsau et al., 1992). Other pathway would be to utilize carbohydrates as a carbon source for fatty acid biosynthesis, which has been associated with acid tolerance in *Lactobacillus bulgaricus* (Fernandez et al., 2008). In this context, it is speculated that when pH is below 3, glucose/fructose transporter system of *L. plantarum* is disrupted or downregulated and thus the ability to utilize sugars as an energy source is limited. In the case of malolactic fermentation, however, deprotonated malic acid can enter a cell through diffusion and is therefore a readily available energy source even when pH is below 3 (Olsen et al., 1991).

Regarding sugar metabolism, exception was made by strain DSM 1055, showing fructose metabolism and various acid stress systems activated at pH 2.7, including trehalose and 4-aminobutyric acid (GABA) formation. GABA is derived from decarboxylation of glutamic acid, followed by transport out of the cell, and the metabolic pathway is used by bacteria to maintain intracellular pH homeostasis (Feehily et al., 2013). Increased GABA production by strain DSM 1055 at natural sea buckthorn pH was therefore possibly an adaption to acid shock.

Ascorbic acid level (1.36 ± 0.02 mM in fresh juice) was significantly higher in fermented juices with starter pH of 3.5 compared to when starter pH was 2.7 (0.70–1.04 and 0.61–0.89 mM, respectively) and especially when compared to the control juice incubated without inoculation (0.25 ± 0.12 mM). Ascorbic acid (or vitamin C) is an unstable food component, and can be degraded during processing and storage when exposed to higher temperatures, moisture, oxygen, light, or changes in pH (Abbas et al., 2012). Earlier, inoculation of cactus cladodes (Filannino, Cavoski, et al., 2016) and fruit-vegetable smoothies (Di Cagno et al., 2011) with lactic acid bacteria reduced the degradation of ascorbic acid during storage.

All in all, while malolactic fermentation was finished in equal fashion at both starter pH 2.7 and 3.5, less sugar and amino acid metabolism was observed at lower pH. On the other hand, at higher starter pH, more secondary metabolite fermentation was present, potentially impacting bitterness or astringency of SBJ (Ferrer-Gallego et al., 2014). When fermentations were started at pH 3.5, ascorbic acid was oxidized at a lower rate compared to control without inoculation or to juices started
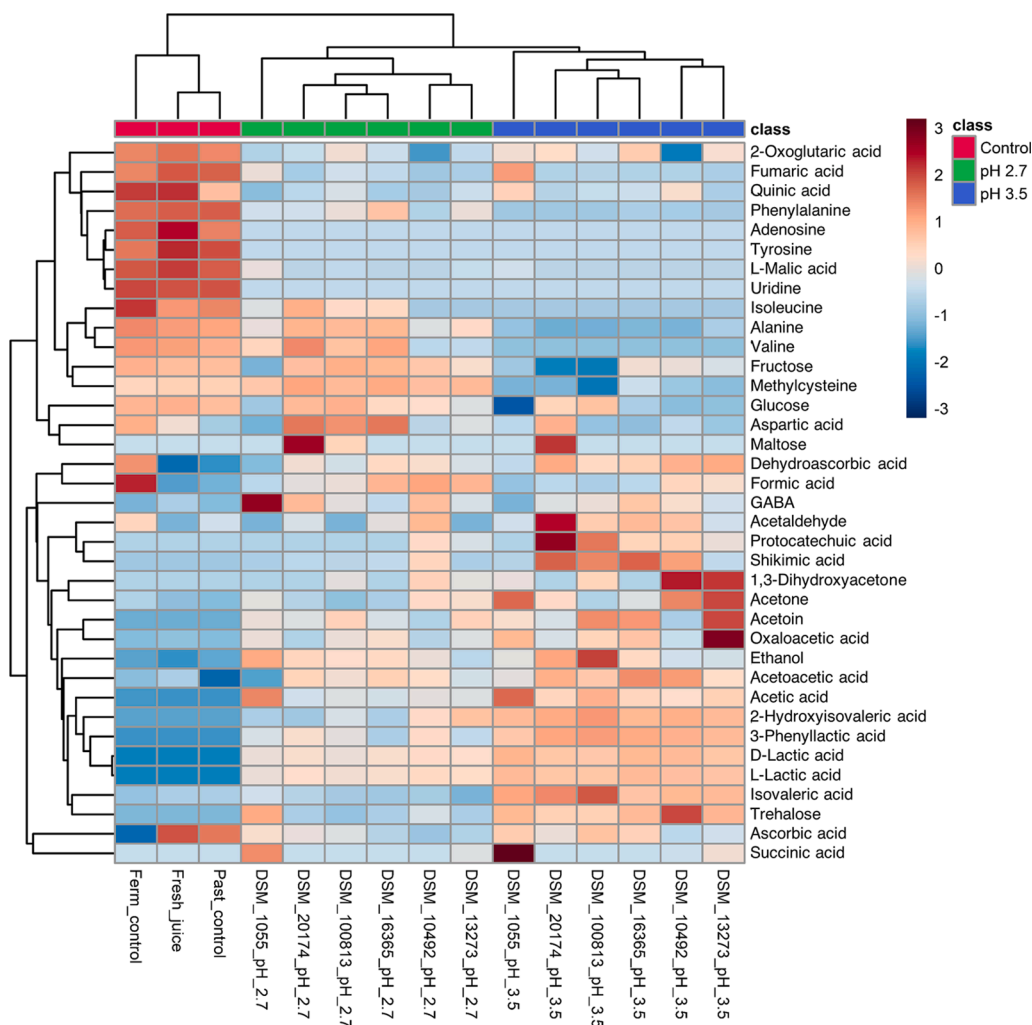
Fig. 2. Hierarchical clustering heatmap analysis of metabolites variations between control and fermented juices with different starter pH (time = 72 h, medium = *CAM*) presented as Euclidean distance. Color scale indicates number of standard deviations from the overall average of the metabolite, with red representing increased and blue representing decreased abundance compared to the mean. (For interpretation of the references to color in this figure legend, the reader is referred to the web version of this article.)

at pH 2.7, which raises the question if pH adjustment together with fermentation could increase storage stability of SBJ. Further work should also focus on the effect of starter pH on sensory value of fermented SBJ to determine optimal starting conditions for fermentation.

3.4. Differences in metabolic activity between L. plantarum strains

In our earlier work, strain-dependent variation in volatile compound profiles after malolactic fermentation of SBJs were observed. In short, the highest producer of volatile acids (acetic acid, 2-hydroxyisovaleric, free fatty acids) and volatile alcohols (3-methyl-1-butanol, benzyl alcohol) was strain DSM 1055 while the highest producer of volatile ketones (acetoin, diacetyl, 2-undecanone) was strain DSM 13273. The lowest level of volatile ketones and acids were produced by strains DSM 100,813 and DSM 16365 (Markkinen et al., 2021). In this work, the target was to illustrate phenotypical variation in metabolic activity when *L. plantarum* is exposed to acidic fruit material. Initially, subset of data (pH = 3.5, fermentation time = 72 h) was fitted into an OPLS-DA model. While groups were separated significantly (CV-ANOVA p-value = 3.8×10^{-36}), the Y-intercepts of R^2Y were over 0.4, showing that the model was not validated, and an unsupervised model (PCA) was used instead to avoid overfitting. Strain DSM 1055 was an outlier in the model (data not shown), showing that the metabolic activity of this strain was distinct from the other tested strains. Due to this, strain DSM 1055 was excluded from the final PCA model (Supplementary Fig. S3). Components 2 and 4 showed clearest separation based on strain, which explained 23.6% and 5.1% of the variation, respectively. Loadings plot

of second component separated strains based on the degree of glucose and fructose metabolism and production of metabolites related to heterofermentative pathways, i.e., acetic acid and ethanol. In the fourth component, strains were separated by compounds related to quinic acid metabolism.

3.4.1. Unique metabolic activity of strain DSM 1055

While other strains had consumed all L-malic acid by 36 h of fermentation, juices fermented with DSM 1055 had residual 24.2 ± 1.7 mM and 4.7 ± 0.2 mM of L-malic acid after 36 and 72 h of fermentation, respectively. In addition, cells of DSM 1055 produced higher levels of succinic and acetic acids compared to other studied strains, however, it should be noted that there was a statistically significant difference in acetic acid formation between cells cultivated in *CAM* and *GEM* ($p <$ 0.05) (see Section 3.6). In addition, DSM 1055 consumed significantly more glucose (Fig. 3) and produced less shikimic and protocatechuic acids compared to the other strains (Fig. 4).

Succinic acid is the final product in the reductive branch of partial citric acid cycle (tricarboxylic acid cycle, TCA) of *L. plantarum* (Tsuji et al., 2013). Another suggested mechanism is degradation of lactic acid with oxaloacetic acid, yielding succinic acid, ATP, formic acid, and CO_2 (Bron et al., 2012). Earlier, accumulation of succinic acid (from citrate) by *L. plantarum C*2 was observed in carrot juice, possibly as a mechanism to save energy by regenerating the cofactor NAD^+ (Filannino, Cagno, et al., 2016). Unlike fermentation of glucose to lactic acid, which is redox balanced, fermentation of glucose *via* pyruvate to acetic acid accumulates NADH (Tsuji et al., 2013), and therefore it is possible that

DSM 1055 uses reductive pathway of TCA to maintain redox homeostasis during fermentation of SBJ.

3.4.2. Phenotypical variation in carbohydrate metabolism

In the second component, strains were separated by sugar metabolism, as glucose utilization was positively correlated in PC-2 while negative correlation was observed with fructose metabolism and formation of acetic acid and ethanol (Supplementary Fig. S3). Closer observation suggested that strains DSM 10492 and DSM 13273 preferred to ferment glucose while strains DSM 100813 and DSM 20174 preferred fructose (Fig. 3). Activating the heterofermentative pathway resulted in the formation of significantly more acetic acid, ethanol, and acetoin by DSM 100813 compared to the other strains. Similar to succinic acid production by strain DSM 1055, increased formation of ethanol by strain DSM 100813 was possibly a mechanism to consume extra NADH formed in acetic acid production.

The highest contents of acetoin, ketone with a buttery and caramel flavor, were detected in juices fermented with DSM 13273 (0.057 ± 0.00 mM). A strong positive correlation between levels of oxaloacetic acid and acetoin ($r = 0.61$) suggests that acetoin was produced from L-malic acid *via* oxaloacetic acid. However, it is not clear how the NADH cofactor is balanced by *L. plantarum* in this pathway, as *L. plantarum* typically lacks the enzyme to reduce acetoin to 2,3-butanediol (Huang et al., 2020).

3.4.3. Strain-dependent differences in quinic acid metabolism

In the fourth component of PCA, strains were separated based on quinic acid metabolism (Supplementary Fig. S3). While there were no statistically significant differences in quinic acid utilization between

L. plantarum strains used in this work, with a reduction from 56.7 ± 0.4 mM in fresh juice to 50.5 ± 2.0 mM in fermented juice on average, the fate of the consumed quinic acid varied significantly between strains (Fig. 4). In this work we suggest that *L. plantarum* metabolized quinic acid in SBJ through two separate pathways, into shikimic acid and 3,4,5-OH-CHCA (reductive pathway), or into protocatechuic acid and catechol (oxidative pathway), with 3-dehydroshikimic acid as intermediate in both cases. The quinic acid metabolism pathways of *L. plantarum* have been described earlier (Whiting & Coggins, 1971, 1974).

Reductive route of quinic acid metabolism was active in strains DSM 100812, DSM 10492, DSM 16365, and DSM 20174, which increased the content of shikimic acid from 0.1 to up to 1.5 mM in SBJ during fermentation, however, significantly lower amounts (<0.3 mM) were detected in juices fermented with strains DSM 1055 and DSM 13273. However, the latter strain further reduced shikimic acid to 3,4,5-OH-CHCA. In earlier work, 3,4-OH-CHCA was reported as the final product in the reductive pathway of quinic acid metabolism of *L. plantarum* (Whiting and Coggins, 1971), however, this metabolite was not detected in our work. As far as the authors are aware, this is the first report where 3,4,5-OH-CHCA is found as a significant quinic acid metabolite by *L. plantarum*. Oxidative route of quinic acid metabolism was particularly present in strains DSM 20174, DSM 13273, and DSM 100813 which metabolized quinic acid assumingly *via* 3-dehydroshikimic acid to protocatechuic acid. While Whiting and Coggins (1971) presented catechol as the end product of this pathway, here only strain DSM 13273 decarboxylated protocatechuic acid into catechol.

Interestingly, while quinic acid content was decreased by strain DSM 1055 in equal amount compared to other strains (Fig. 4), only moderate increase in shikimic and protocatechuic acid contents were observed.

Fig. 3. Suggested metabolic pathways in *L. plantarum* during fermentation of sea buckthorn juice. The bar plots represent comparison of concentrations or normalized peak areas of metabolites associated with homo- and heterofermentative pathways between fresh juice, juice fermented without inoculation, and juices fermented with different *L. plantarum* strains. Letters a–f mark a statistically significant difference over different juices with one-way ANOVA and Tukey's HSD test of significance ($p < 0.05$). Results are average $\pm$ standard deviation.
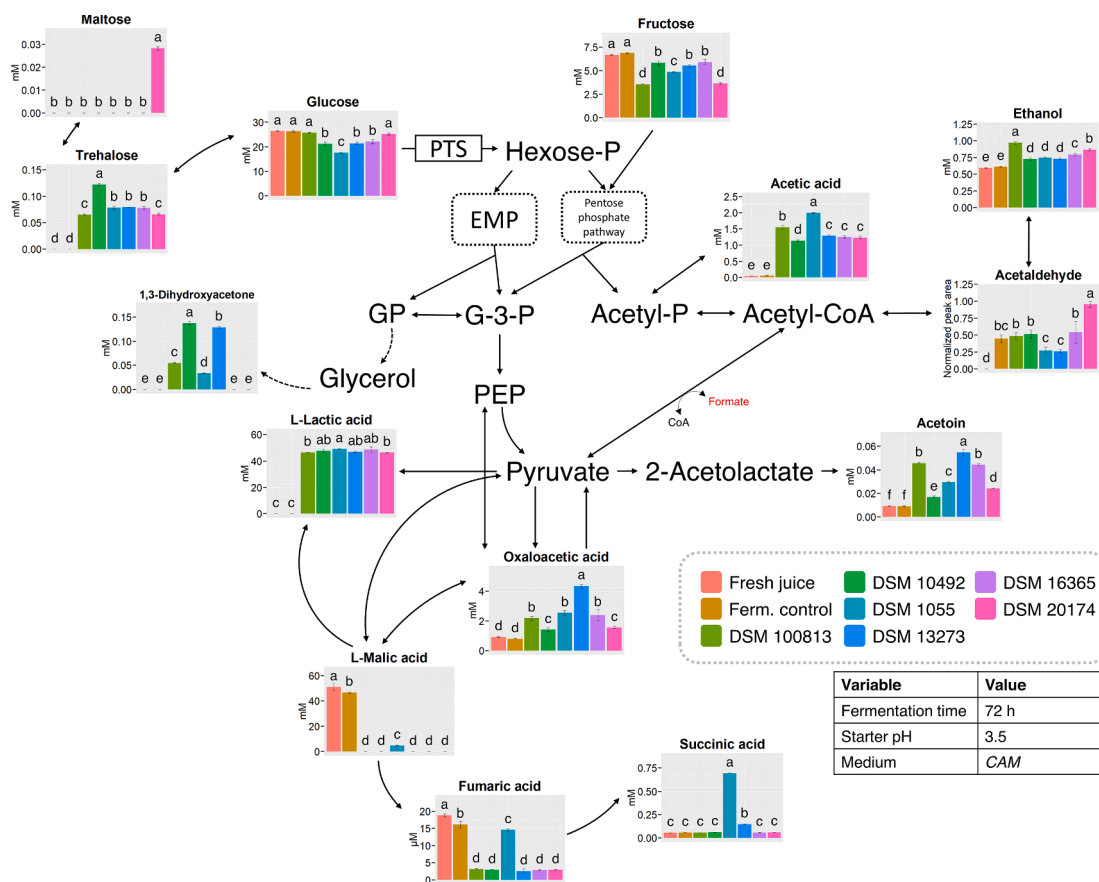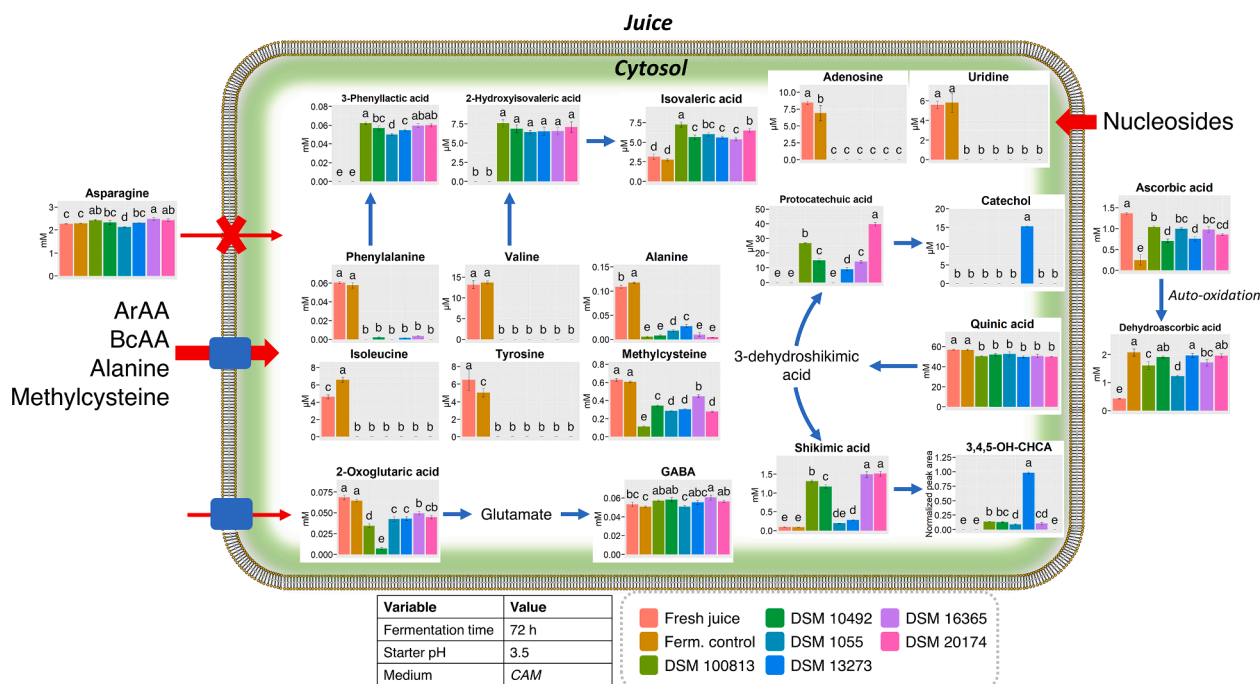
Fig. 4. Suggested metabolic pathways in *L. plantarum* during fermentation of sea buckthorn juice. The bar plots represent comparison of concentrations or normalized peak areas of metabolites associated with amino acids, quinic acid, ascorbic acid, and nucleosides between fresh juice, juice fermented without inoculation, and juices fermented with different L. plantarum strains. Letters a–e mark a statistically significant difference over different juices with one-way ANOVA and Tukey's HSD test of significance (p < 0.05). Results are average ± standard deviation.

One possible explanation is that the strain has utilized shikimic acid as a substrate for aromatic amino acid biosynthesis rather than releasing it to the extracellular space (Filannino, Cagno, et al., 2016).

Some heterofermentative *Lactobacillus* species utilize hydroxycinnamic acids as additional electron acceptors, providing an energetic advantage to allow increased metabolic flux of acetate phosphate to acetic acid (instead of ethanol) to yield ATP (Filannino, Gobbetti, et al., 2014). Further analysis suggested that also in this work several of the tested *L. plantaum* strains utilized quinic acid for acetic acid production (see Section 3.5).

3.4.4. Other metabolites

Lactic acid bacteria are in general unable to produce 2-oxoglutaric acid through TCA and therefore glutamic acid auxotrophy is widespread among *Lactobacillus* spp., including *L. plantarum* (Teusink et al., 2005). As no glutamic acid was detected from fresh SBJ, it was an unexpected result that only strain DSM 10492 effectively utilized 2-oxoglutaric acid present in SBJ (Fig. 4). Whether there was an unidentified source of glutamic acid (such as oligopeptides) or 2-oxoglutaric acid present in SBJ remains to be elucidated.

Strains DSM 10492 and DSM 13273 produced significantly higher content of dihydroxyacetone (DHA) (0.13–0.14 mM) compared to other strains (0–0.05 mM) (Fig. 3). No clear substrate for DHA was detected from the metabolic profile of fresh or fermented SBJ. One potential source would be dihydroxyacetone-phosphate (DHAP) which is produced as intermediate in glycolysis from β-D-fructose 1,6-bisphosphate or from glyceraldehyde-3-phosphate (Fig. 3). While gene for DHA kinase (*dhaK*) have been detected from *L. plantarum*, it is assumed that the enzyme catalyzes the formation of DHAP from DHA, not *vice versa* (Doi, 2019), making DHAP an unlikely source. On the other hand, DHA can be produced by glycerol dehydrogenase enzyme (Doi, 2019), encoded by the gene *gldA* in *L. plantarum* (accession number: WP_021338259). The gene is not widespread in *L. plantarum* (Doi, 2019), which could explain why DHA was not produced by all the tested strains. While no glycerol was detected in fermented SBJ, the substrate could have remained intracellular and only DHA was released after oxidation.

L. plantarum produced trehalose up to 0.13 mM during fermentation of SBJ, strain DSM 10492 producing significantly more than the other studied strains (Fig. 3). In addition, strain DSM 20174 further converted trehalose to maltose. Trehalose and maltose function as multi-stress protectors due to high water holding capacity and thus help to stabilize microbial cell wall under e.g. acid or osmotic stress. Recently, accumulation of trehalose by *L. plantarum* was reported under ethanol stress (Chen et al., 2020). While trehalose is typically biosynthesized in bacteria from glucose and UDP-glucose with trehalose-phosphate as intermediate (Ruhal et al., 2013), no established pathway of trehalose biosynthesis in *L. plantarum* has been discovered.

3.5. Evolution of metabolic profile of sea buckthorn juice during fermentation

Incubation time is an essential factor in fermentation to produce foods with optimal organoleptic and functional properties (Sharma et al., 2020). In this work, we compared change in concentrations of selected metabolites between 0 and 36 h (referred later as *phase I*) and 36–72 h of fermentation (*phase II*) (Fig. 5, Supplementary Fig. S4 and S5). While the majority of the identified compounds were affected by fermentation, compounds that showed little or no change during fermentation include trigonelline, asparagine, ethyl glucose, *myo*-inositol, and ʟ-quebrachitol (Supplementary Fig. S4).

From Figs. 5 and 6 it can be observed that ʟ-malic acid, amino acids, and nucleosides were utilized early in fermentation, with over 70–100% of the total reduction occurring during *phase I*. In accordance with this, majority of ʟ-lactic acid, 2-hydroxyisovaleric acid, and 3-PLA were produced at the same time. To lesser extent, higher abundance of ethanol, acetoin, oxaloacetic acid, and dihydroxyacetone were also formed during *phase I* compared to *phase II*.

Fermentation of sugars was more constant on average during fermentation. It should be noted, however, that results of glucose and fructose showed high standard deviation in Fig. 6 due to strain-dependent differences in sugar metabolism (Fig. 3). For example, the highest fructose utilizers strains DSM 20174 and DSM 100813 consumed
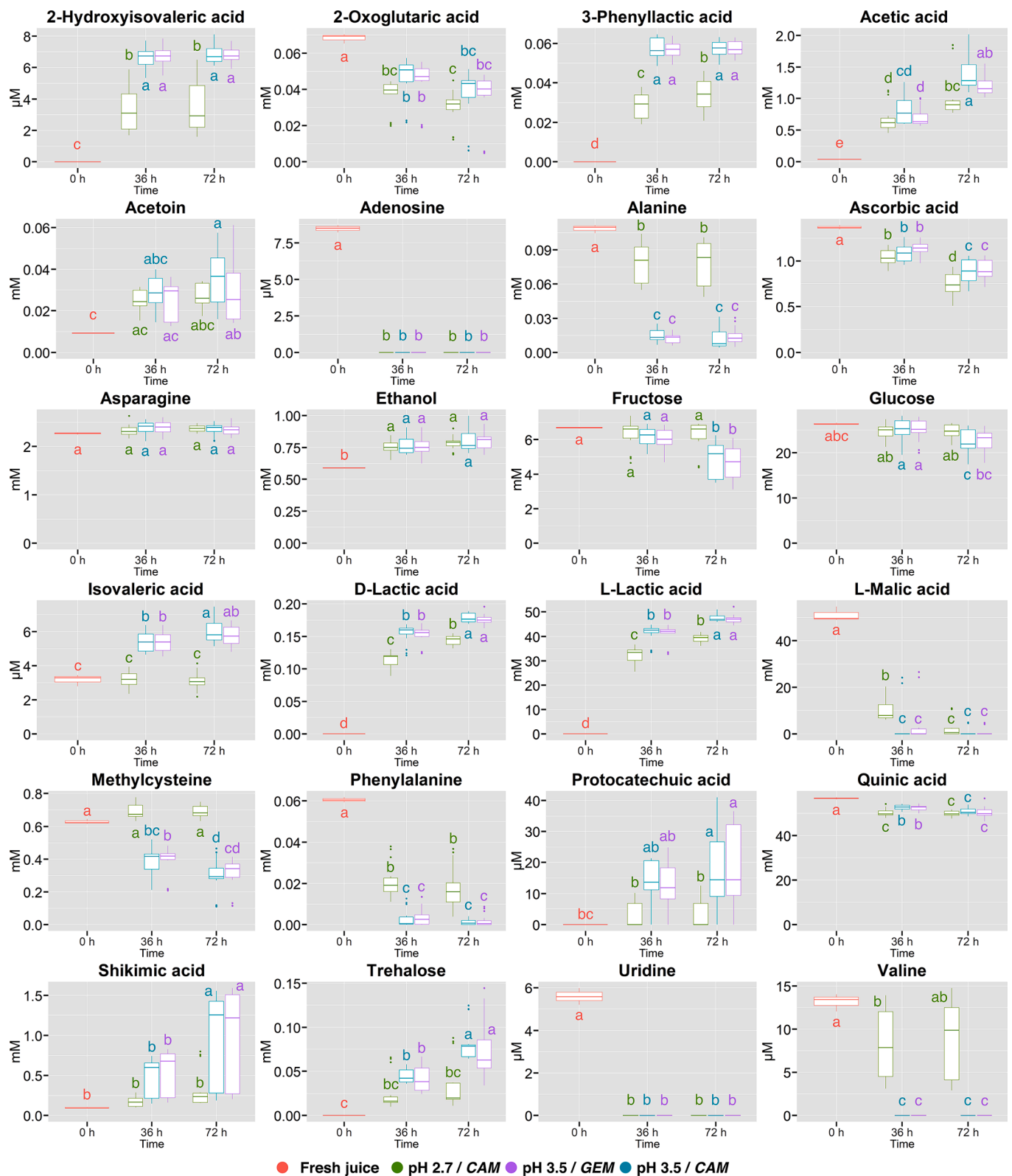
Fig. 5. Evolution of the metabolite concentrations during fermentation in sea buckthorn juices with results aggregated based on starter pH and growth medium and presented as box-and-whiskers plots. Letters a–e mark statistically significant difference over time, starter pH and medium with one-way ANOVA and Tukey's HSD test of significance (p < 0.05).

0.73–1.17 mM of fructose in SBJ during *phase I* but there was two-fold increase in consumption (2.03–2.31 mM) during *phase II*. On the other hand, strain DSM 1055, highest glucose utilizer (Fig. 3), consumed the majority of glucose (73–77% out of total decrease of 8.57 mM) during

phase I. Moderate glucose utilizers, DSM 13273 and DSM 10492 consumed 30.3–34.1% and 47.3–58.7% out of total decrease 5.06 and 4.24 mM, respectively, during *phase I*. This result suggests that strain DSM 1055 utilized L-malic acid and glucose simultaneously as energy

A

Metabolite	0 - 36 h	36 - 72 h
Fructose	49.1 ± 26.4	50.9 ± 26.4
Glucose	53.2 ± 19.3	46.8 ± 19.3
Ascorbic acid	57.3 ± 10.7	42.7 ± 10.7
Quinic acid	68.4 ± 14.1	31.6 ± 14.1
2-Oxoglutaric acid	72.3 ± 6.4	27.7 ± 6.4
Methylcysteine	72.4 ± 9.2	27.6 ± 9.2
L-Malic acid	92.5 ± 16.5	7.5 ± 16.5
Alanine	95.5 ± 3.6	4.5 ± 3.6
Phenylalanine	97 ± 4.1	3 ± 4.1
Adenosine	100 ± 0	0 ± 0
Isoleucine	100 ± 0	0 ± 0
Tyrosine	100 ± 0	0 ± 0
Uridine	100 ± 0	0 ± 0
Valine	100 ± 0	0 ± 0

Relative decrease / Total change during fermentation

B

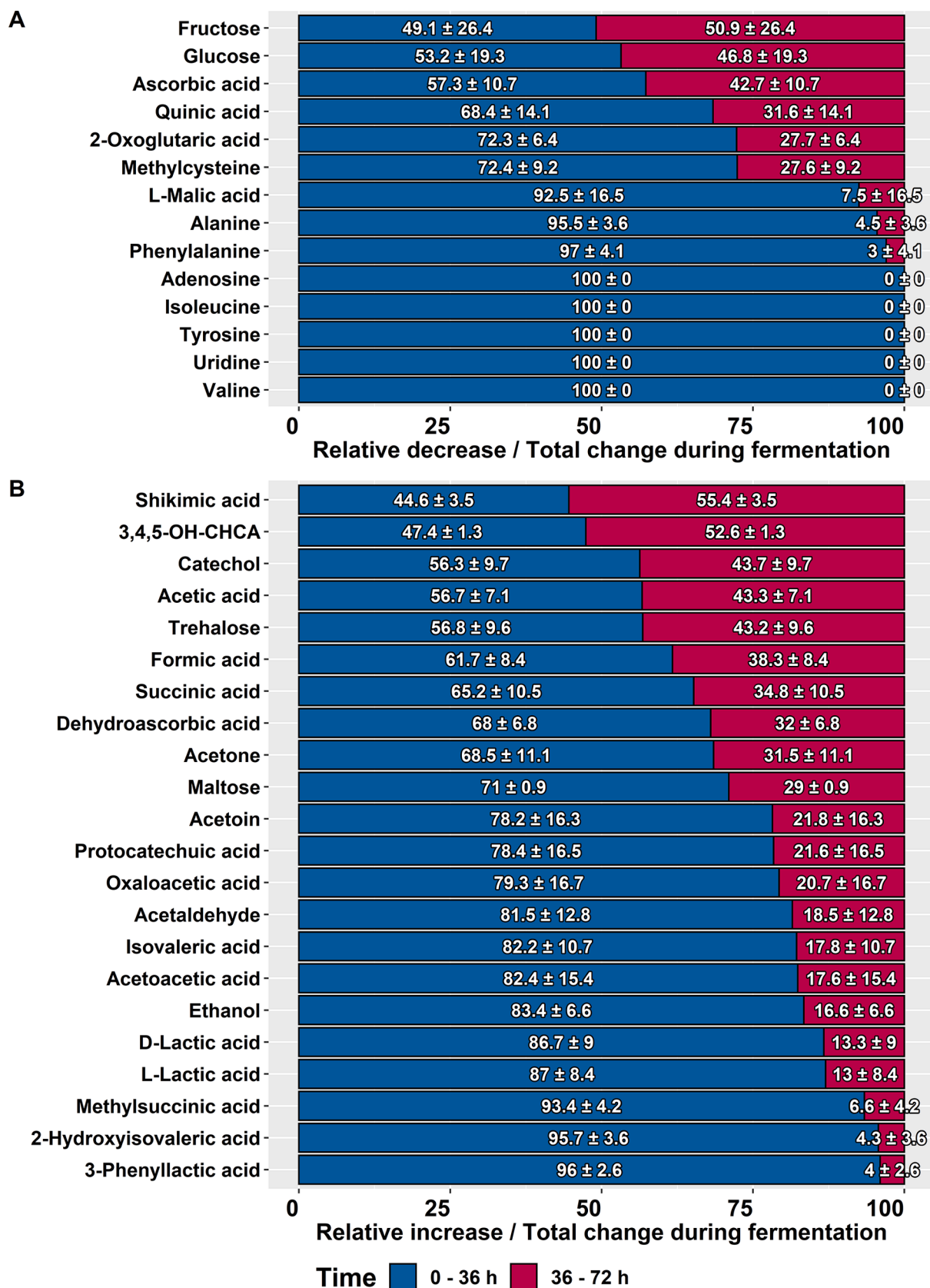| Metabolite	0 - 36 h	36 - 72 h
Shikimic acid	44.6 ± 3.5	55.4 ± 3.5
3,4,5-OH-CHCA	47.4 ± 1.3	52.6 ± 1.3
Catechol	56.3 ± 9.7	43.7 ± 9.7
Acetic acid	56.7 ± 7.1	43.3 ± 7.1
Trehalose	56.8 ± 9.6	43.2 ± 9.6
Formic acid	61.7 ± 8.4	38.3 ± 8.4
Succinic acid	65.2 ± 10.5	34.8 ± 10.5
Dehydroascorbic acid	68 ± 6.8	32 ± 6.8
Acetone	68.5 ± 11.1	31.5 ± 11.1
Maltose	71 ± 0.9	29 ± 0.9
Acetoin	78.2 ± 16.3	21.8 ± 16.3
Protocatechuic acid	78.4 ± 16.5	21.6 ± 16.5
Oxaloacetic acid	79.3 ± 16.7	20.7 ± 16.7
Acetaldehyde	81.5 ± 12.8	18.5 ± 12.8
Isovaleric acid	82.2 ± 10.7	17.8 ± 10.7
Acetoacetic acid	82.4 ± 15.4	17.6 ± 15.4
Ethanol	83.4 ± 6.6	16.6 ± 6.6
D-Lactic acid	86.7 ± 9	13.3 ± 9
L-Lactic acid	87 ± 8.4	13 ± 8.4
Methylsuccinic acid	93.4 ± 4.2	6.6 ± 4.2
2-Hydroxyisovaleric acid	95.7 ± 3.6	4.3 ± 3.6
3-Phenyllactic acid	96 ± 2.6	4 ± 2.6

Relative increase / Total change during fermentation

Time ■ 0 - 36 h ■ 36 - 72 h

Fig. 6. Relative increase or decrease (%) in concentration of selected metabolites (average ± standard deviation) during fermentation. Only juices with starter pH 3.5 were included to comparison. To remove data points where there was no reduction or forming of the metabolite, data was algorithmically filtered to exclude data points where change was <5, 10 or 15% of the maximum amount when maximum amount was more than 10 mM, between 1 and 10 mM or <1 mM, respectively.

sources, while strains DSM 20174, DSM 100813, and DSM 13273 increased sugar fermentation once L-malic acid was exhausted.

Acetic acid, trehalose and quinic acid metabolites (shikimic acid, 3,4,5-OH-CHCA, catechol) were formed at nearly equal rate during *phase I* and *phase II* (Fig. 5). While most of the studied strains produced majority ($> 80\%$) of protocatechuic acid during *phase I*, highest producer of protocatechuic acid, strain DSM 20174, formed 51.2–53.2% (out of total 0.04 mM) of the compound during *phase II*.

Energy sources, nucleosides, and free amino acids, especially branched chain amino acids and phenylalanine, are essential for cell functions and growth of *L. plantarum* (Ma et al., 2016) and were therefore consumed rapidly already early in fermentation. In contrast, free amino acid content of bog bilberry juice was increased from 23 up to 95 mg/L during fermentation with *L. plantarum*, possibly due to proteolytic activity (Wei et al., 2018).

Metabolism of quinic acid, which occurred throughout the fermentation, was associated with the maintenance of redox homeostasis (Section 3.4.3). The very strong correlation between the concentrations of acetic acid and shikimic acid in fermented juices ($r = 0.83$) suggests that *L. plantarum* used quinic acid to recycle NADH surplus from ATP production *via* heterofermentative pathway. Exception was made by strain DSM 1055 which utilized reductive pathway of TCA to allow acetic acid formation (see Section 3.4.1).

It can be summarized that if the target of malolactic fermentation is solely to convert L-malic to D/L-lactic acid to reduce acidity, shorter fermentation times should be preferred. In addition, our earlier work revealed that juices fermented for 36 h instead of 72 h retained higher levels of volatile esters and terpenes important for natural aroma of sea buckthorn (Markkinen et al., 2021). However, if the target is to impact bitter or astringent secondary metabolites (such as quinic acid), increasing fermentation time is required to activate metabolic pathways related to maintenance or survival in the stationary phase. In this case, acidity is likely increased after exhausting of L-malic acid due to fermentation of sugars and subsequent formation of lactic and acetic acids.

3.6. Effect of acclimation on metabolic activity of L. plantarum

Besides the differences in the metabolic profiles of SBJ dependent on starter pH and bacterial strain, it was also investigated if acclimation had an impact on the metabolism of *L. plantarum*. As the cells grown in *GEM* were unable to ferment SBJ at natural pH, only juice samples with starter pH of 3.5 could be utilized for the comparison.

In general, the metabolic activity of *L. plantarum* was highly homologous between cells grown in either *GEM* or *CAM*, similar to our earlier report (Markkinen et al., 2021). However, there were statistically significant differences in the concentrations of the selected individual metabolites that were further dependent on the strain used for the fermentation (Supplementary Fig. S5, S6).

The production of acetic acid, succinic acid, acetoin, and trehalose by the strain DSM 1055 was twofold by cells cultivated in *CAM* compared to the cells grown in *GEM*. This result was in line with the earlier suggestion that the strain DSM 1055 utilizes TCA for acetic acid production. The difference with the highest magnitude was observed in the production of dihydroxyacetone by strains DSM 100813 and DSM 1055, as almost no production was observed when cells had been grown in *GEM* compared to the production by cells grown in *CAM* (Supplementary Fig. S5). One possibility is that acclimation has led to the increased expression of genes related to stress adaptation, heterofermentative pathways, and TCA prior to inoculation to SBJ which in turn has increased the production of downstream metabolites related to these pathways, including acetic acid, acetoin, and succinic acid. As a summary, acclimation the cell culture can be used as an alternative approach to pH adjustment to improve fermentation of SBJ or other highly acidic juices since there was no compromise in biomass formation during the starter culture production (Markkinen et al., 2021), and in this study, no

unwanted metabolic activity was detected with cells grown in *CAM*.

4. Conclusions

The work set out to reveal phenotypical variation in metabolic activity between various strains of *L. plantarum* in fermentation of acidic fruit material. A total of 46 metabolites were identified from the fresh and fermented SBJ, including various sugars, amino acids, organic acids, ketones, nucleosides as well as one alkaloid, trigonelline. Regarding nutritional requirements of *L. plantarum*, SBJ was a source for energy and carbon (malic acid, fructose, glucose), for essential amino acids or necessary precursors (apart from methionine), and for purine (adenosine).

To summarize, NMR proved a suitable method for holistic analysis of lactic acid fermented fruit material, allowing optimization of malolactic fermentation with *L. plantarum* of SBJ. If malolactic fermentation is used primarily for deacidification purposes, shorter fermentation times, lower starter pH, and less acid producing strains such as DSM 16365 or DSM 20174 should be used. However, if secondary metabolites are also the intended target for modification during the fermentation (for example, quinic acid or phenolic compounds), or if there is intent to also improve the microbial or oxidative stability of the material, higher starter pH and longer fermentation times could be considered. In addition, the analysis revealed that various metabolic pathways activated differently between strains related to homo- and heterofermentation, stress-associated compounds, quinic acid metabolism, and tricarboxylic acid cycle. One possible explanation to differentiated metabolism was to consume excess NADH produced from acetate and acetoin production through separate mechanisms: strain DSM 13273 generated 3,4,5-OH-CHCA (from quinic acid) while strain DSM 100813 used ethanol and strain DSM 1055 succinic acid as electron acceptors.

CRediT authorship contribution statement

N. Markkinen: Conceptualization, Methodology, Validation, Formal analysis, Investigation, Writing - original draft, Visualization, Funding acquisition, Project administration. **R. Pariyani:** Conceptualization, Methodology, Validation, Investigation, Writing - review & editing. **J. Jokioja:** Methodology, Investigation, Writing - review & editing. **M. Kortesniemi:** Methodology, Writing - review & editing, Formal analysis. **O. Laaksonen:** Conceptualization, Writing - review & editing, Supervision, Project administration. **B. Yang:** Conceptualization, Writing - review & editing, Supervision, Funding acquisition, Project administration, Resources.

Declaration of Competing Interest

The authors declare that they have no known competing financial interests or personal relationships that could have appeared to influence the work reported in this paper.

Acknowledgements

Appendix A. Supplementary data

Supplementary data to this article can be found online at https://doi.org/10.1016/j.foodchem.2021.130630.

References

Abbas, S., Da Wei, C., Hayat, K., & Xiaoming, Z. (2012). Ascorbic acid: Microencapsulation techniques and trends—A review. *Food Reviews International, 28*(4), 343–374. https://doi.org/10.1080/87559129.2011.635390.

Bal, L. M., Meda, V., Naik, S. N., & Satya, S. (2011). Sea buckthorn berries: A potential source of valuable nutrients for nutraceuticals and cosmoceuticals. *Food Research International, 44*(7), 1718–1727. https://doi.org/10.1016/j.foodres.2011.03.002.

Brizuela, N., Tymczyszyn, E. E., Semorile, L. C., Valdes La Hens, D., Delfederico, L., Hollmann, A., & Bravo-Ferrada, B. (2019). *Lactobacillus plantarum* as a malolactic starter culture in winemaking: A new (old) player? *Electronic Journal of Biotechnology, 38*, 10–18. https://doi.org/10.1016/j.ejbt.2018.12.002.

Bron, P. A., Wels, M., Bongers, R. S., van Bokhorst-van de Veen, H., Wiersma, A., Overmars, L., … Driessen, A. (2012). Transcriptomes reveal genetic signatures underlying physiological variations imposed by different fermentation conditions in *Lactobacillus plantarum*. *PLoS ONE, 7*(7), e38720. https://doi.org/10.1371/journal.pone.0038720.

Chen, X., Wang, T., Jin, M., Tan, Y., Liu, L., Liu, L., … Du, P. (2020). Metabolomics analysis of growth inhibition of *Lactobacillus plantarum* under ethanol stress. *International Journal of Food Science & Technology, 55*(11), 3441–3454. https://doi.org/10.1111/ijfs.v55.1110.1111/ijfs.14677.

Chong, J., & Xia, J. (2018). MetaboAnalystR: An R package for flexible and reproducible analysis of metabolomics data. *Bioinformatics (Oxford, England), 34*(24), 4313–4314. https://doi.org/10.1093/bioinformatics/bty528.

Dal Bello, F., Clarke, C. I., Ryan, L. A. M., Ulmer, H., Schober, T. J., Ström, K., … Arendt, E. K. (2007). Improvement of the quality and shelf life of wheat bread by fermentation with the antifungal strain *Lactobacillus plantarum* FST 1.7. *Journal of Cereal Science, 45*(3), 309–318. https://doi.org/10.1016/j.jcs.2006.09.004.

Di Cagno, R., Minervini, G., Rizzello, C. G., De Angelis, M., & Gobbetti, M. (2011). Effect of lactic acid fermentation on antioxidant, texture, color and sensory properties of red and green smoothies. *Food Microbiology, 28*(5), 1062–1071. https://doi.org/10.1016/j.fm.2011.02.011.

Doi, Y. (2019). Glycerol metabolism and its regulation in lactic acid bacteria. *Applied Microbiology and Biotechnology, 103*(13), 5079–5093. https://doi.org/10.1007/s00253-019-09830-y.

Duarte, I. F., Delgadillo, I., & Gil, A. M. (2006). Study of natural mango juice spoilage and microbial contamination with *Penicillium expansum* by high resolution 1H NMR spectroscopy. *Food Chemistry, 96*(2), 313–324. https://doi.org/10.1016/j.foodchem.2005.04.008.

Feehily, C., & Karatzas, K. A. G. (2013). Role of glutamate metabolism in bacterial responses towards acid and other stresses. *Journal of Applied Microbiology, 114*(1), 11–24. https://doi.org/10.1111/j.1365-2672.2012.05434.x.

Fernandez, Annabelle, Ogawa, Jun, Penaud, Stéphanie, Boudebbouze, Samira, Ehrlich, Dusko, van de Guchte, Maarten, & Maguin, Emmanuelle (2008). Rerouting of pyruvate metabolism during acid adaptation in *Lactobacillus bulgaricus*. *Proteomics, 8*(15), 3154–3163. https://doi.org/10.1002/pmic.200700974.

Ferrer-Gallego, R., Hernández-Hierro, J. M., Rivas-Gonzalo, J. C., & Escribano-Bailón, M. T. (2014). Sensory evaluation of bitterness and astringency sub-qualities of wine phenolic compounds: Synergistic effect and modulation by aromas. *Food Research International, 62*, 1100–1107. https://doi.org/10.1016/j.foodres.2014.05.049.

Filannino, P., Cagno, R. D., Crecchio, C., Virgilio, C. D., Angelis, M. D., & Gobbetti, M. (2016). Transcriptional reprogramming and phenotypic switching associated with the adaptation of *Lactobacillus plantarum* C2 to plant niches. *Scientific Reports, 6*(1), 1–16. https://doi.org/10.1038/srep27392.

Filannino, P., Cardinali, G., Rizzello, C. G., Buchin, S., De Angelis, M., Gobbetti, M., & Di Cagno, R. (2014). Metabolic Responses of *Lactobacillus plantarum* Strains during Fermentation and Storage of Vegetable and Fruit Juices. *Applied and Environmental Microbiology, 80*(7), 2206–2215. https://doi.org/10.1128/AEM.03885-13.

Filannino, P., Cavoski, I., Thlien, N., Vincentini, O., Angelis, M. D., Silano, M., … Cagno, R. D. (2016). Lactic Acid Fermentation of Cactus Cladodes (*Opuntia ficus-indica* L.) Generates Flavonoid Derivatives with Antioxidant and Anti-Inflammatory Properties. *PLoS ONE, 11*(3), Article e0152575. https://doi.org/10.1371/journal.pone.0152575.

Filannino, P., Gobbetti, M., De Angelis, M., & Di Cagno, R. (2014). Hydroxycinnamic Acids Used as External Acceptors of Electrons: An Energetic Advantage for Strictly Heterofermentative Lactic Acid Bacteria. *Applied and Environmental Microbiology, 80*(24), 7574–7582. https://doi.org/10.1128/AEM.02413-14.

Hong, Y.-S. (2011). NMR-based metabolomics in wine science: NMR in wine science. *Magnetic Resonance in Chemistry, 49*, S13–S21. https://doi.org/10.1002/mrc.2832.

Huang, T., Xiong, T., Peng, Z., Xiao, Y., Liu, Z., Hu, M., & Xie, M. (2020). Genomic analysis revealed adaptive mechanism to plant-related fermentation of *Lactobacillus plantarum* NCU116 and *Lactobacillus* spp. *Genomics, 112*(1), 703–711. https://doi.org/10.1016/j.ygeno.2019.05.004.

Kortesniemi, M., Sinkkonen, J., Yang, B., & Kallio, H. (2014). 1H NMR spectroscopy reveals the effect of genotype and growth conditions on composition of sea buckthorn (*Hippophaë rhamnoides* L.) berries. *Food Chemistry, 147*, 138–146. https://doi.org/10.1016/j.foodchem.2013.09.133.

Kortesniemi, M., Sinkkonen, J., Yang, B., & Kallio, H. (2017). NMR metabolomics demonstrates phenotypic plasticity of sea buckthorn (*Hippophaë rhamnoides*) berries with respect to growth conditions in Finland and Canada. *Food Chemistry, 219*, 139–147. https://doi.org/10.1016/j.foodchem.2016.09.125.

Lavermicocca, P., Valerio, F., & Visconti, A. (2003). Antifungal activity of phenyllactic acid against molds isolated from bakery products. *Applied and Environmental Microbiology, 69*(1), 634–640. https://doi.org/10.1128/AEM.69.1.634-640.2003.

Li, W., Ruan, C.-J., Teixeira da Silva, J. A., Guo, H., & Zhao, C.-E. (2013). NMR metabolomics of berry quality in sea buckthorn (*Hippophae* L.). *Molecular Breeding, 31*(1), 57–67. https://doi.org/10.1007/s11032-012-9768-x.

Liu, Yue, Fan, Gang, Zhang, Jing, Zhang, Yi, Li, Jingjian, Xiong, Chao, … Lai, Xianrong (2017). Metabolic discrimination of sea buckthorn from different *Hippophaë* species by 1 H NMR based metabolomics. *Scientific Reports, 7*(1). https://doi.org/10.1038/s41598-017-01722-3.

Ma, C., Cheng, G., Liu, Z., Gong, G., & Chen, Z. (2016). Determination of the essential nutrients required for milk fermentation by *Lactobacillus plantarum*. *LWT – Food Science and Technology, 65*, 884–889. https://doi.org/10.1016/j.lwt.2015.09.003.

Markkinen, N., Laaksonen, O., Nahku, R., Kuldjärv, R., & Yang, B. (2019). Impact of lactic acid fermentation on acids, sugars, and phenolic compounds in black chokeberry and sea buckthorn juices. *Food Chemistry, 286*, 204–215. https://doi.org/10.1016/j.foodchem.2019.01.189.

Markkinen, Niko, Laaksonen, Oskar, & Yang, Baoru (2021). Impact of malolactic fermentation with *Lactobacillus plantarum* on volatile compounds of sea buckthorn juice. *European Food Research and Technology, 247*(3), 719–736. https://doi.org/10.1007/s00217-020-03660-3.

Muhialdin, Belal J., Kadum, Hana, & Meor Hussin, Anis Shobirin (2021). Metabolomics profiling of fermented cantaloupe juice and the potential application to extend the shelf life of fresh cantaloupe juice for six months at 8 °C. *Food Control, 120*, 107555. https://doi.org/10.1016/j.foodcont.2020.107555.

Muhialdin, Belal J., Kadum, Hana, Zarei, Mohammad, & Meor Hussin, Anis Shobirin (2020). Effects of metabolite changes during lacto-fermentation on the biological activity and consumer acceptability for dragon fruit juice. *LWT, 121*, 108992. https://doi.org/10.1016/j.lwt.2019.108992.

Olsen, E. B., Russell, J. B., & Henick-Kling, T. (1991). Electrogenic L-malate transport by *Lactobacillus plantarum*: A basis for energy derivation from malolactic fermentation. *Journal of Bacteriology, 173*(19), 6199–6206. https://doi.org/10.1128/JB.173.19.6199-6206.1991.

R Core Team. (2021). *R: A language and environment for statistical computing. (4.0.4)*. [Computer software].

Ruhal, Rohit, Kataria, Rashmi, & Choudhury, Bijan (2013). Trends in bacterial trehalose metabolism and significant nodes of metabolic pathway in the direction of trehalose accumulation. *Microbial Biotechnology, 6*(5), 493–502. https://doi.org/10.1111/1751-7915.12029.

Sharma, R., Garg, P., Kumar, P., Bhatia, S. K., & Kulshrestha, S. (2020). Microbial fermentation and its role in quality improvement of fermented foods. *Fermentation, 6*(4), 106. https://doi.org/10.3390/fermentation6040106.

Teusink, B., van Enckevort, F. H. J., Francke, C., Wiersma, A., Wegkamp, A., Smid, E. J., & Siezen, R. J. (2005). In Silico reconstruction of the metabolic pathways of *Lactobacillus plantarum*: Comparing predictions of nutrient requirements with those from growth experiments. *Applied and Environmental Microbiology, 71*(11), 7253–7262. https://doi.org/10.1128/AEM.71.11.7253-7262.2005.

Tomita, Satoru, Saito, Katsuichi, Nakamura, Toshihide, Sekiyama, Yasuyo, Kikuchi, Jun, & Nychas, George-John (2017). Rapid discrimination of strain-dependent fermentation characteristics among *Lactobacillus* strains by NMR-based metabolomics of fermented vegetable juice. *PLoS ONE, 12*(7), e0182229. https://doi.org/10.1371/journal.pone.0182229.

Tsau, Jya-Li, Guffanti, Arthur A., & Montville, Thomas J. (1992). Conversion of Pyruvate to Acetoin Helps To Maintain pH Homeostasis in *Lactobacillus plantarum*. *Applied and Environmental Microbiology, 58*(3), 891–894.

Tsuji, A., Okada, S., Hols, P., & Satoh, E. (2013). Metabolic engineering of *Lactobacillus plantarum* for succinic acid production through activation of the reductive branch of the tricarboxylic acid cycle. *Enzyme and Microbial Technology, 53*(2), 97–103. https://doi.org/10.1016/j.enzmictec.2013.04.008.

Wei, Ming, Wang, Shaoyang, Gu, Pan, Ouyang, Xiaoyu, Liu, Shuxun, Li, Yiqing, … Zhu, Baoqing (2018). Comparison of physicochemical indexes, amino acids, phenolic compounds and volatile compounds in bog bilberry juice fermented by *Lactobacillus plantarum* under different pH conditions. *Journal of Food Science and Technology, 55*(6), 2240–2250. https://doi.org/10.1007/s13197-018-3141-y.

Whiting, G. C., & Coggins, R. A. (1971). The role of quinate and shikimate in the metabolism of lactobacilli. *Antonie van Leeuwenhoek, 37*(1), 33–49. https://doi.org/10.1007/BF02218465.

Whiting, G. C., & Coggins, R. A. (1974). A new nicotinamide–adenine dinucleotide-dependent hydroaromatic dehydrogenase of *Lactobacillus plantarum* and its role in formation of (–)*t*-3, t-4-dihydroxycyclohexane-c-1-carboxylate. *Biochemical Journal, 141*(1), 35–42. https://doi.org/10.1042/bj1410035.